Journal of Experimental Botany, Vol. 62, No. 15, pp. 5497–5508, 2011
doi:10.1093/jxb/err231 Advance Access publication 24 August, 2011
This paper is available online free of all access charges (see http://jxb.oxfordjournals.org/open_access.html for further details)

Journal of Experimental Botany
www.jxb.oxfordjournals.org

RESEARCH PAPER

Functional effect of grapevine 1-deoxy-D-xylulose 5-phosphate synthase substitution K284N on Muscat flavour formation

Juri Battilana[1,*], Francesco Emanuelli[1], Giorgio Gambino[2], Ivana Gribaudo[2], Flavia Gasperi[3], Paul K. Boss[4] and Maria Stella Grando[1]

[1] Fondazione Edmund Mach, Research and Innovation Centre, Genomic and Biology of Fruit Crops Department, Via Mach, 1, 38010 San Michele all'Adige (TN), Italy
[2] Istituto Virologia Vegetale, CNR Unità Grugliasco, Via Leonardo da Vinci, 44, 10095 Grugliasco (TO), Italy
[3] Fondazione Edmund Mach, Research and Innovation Centre, Food Quality and Nutrition Department, Via Mach, 1, 38010 San Michele all'Adige (TN), Italy
[4] CSIRO Plant Industry, WIC West building Waite Campus, PO Box 350, Glen Osmond, SA 5064, Australia

* To whom correspondence should be addressed. E-mail: juri.battilana@iasma.it

Received 30 March 2011; Revised 15 June 2011; Accepted 27 June 2011

Abstract

Grape berries of Muscat cultivars (*Vitis vinifera* L.) contain high levels of monoterpenols and exhibit a distinct aroma related to this composition of volatiles. A structural gene of the plastidial methyl-erythritol-phosphate (MEP) pathway, 1-deoxy-D-xylulose 5-phosphate synthase (*VvDXS*), was recently suggested as a candidate gene for this trait, having been co-localized with a major quantitative trait locus for linalool, nerol, and geraniol concentrations in berries. In addition, a structured association study discovered a putative causal single nucleotide polymorphism (SNP) responsible for the substitution of a lysine with an asparagine at position 284 of the VvDXS protein, and this SNP was significantly associated with Muscat-flavoured varieties. The significance of this nucleotide difference was investigated by comparing the monoterpene profiles with the expression of *VvDXS* alleles throughout berry development in Moscato Bianco, a cultivar heterozygous for the SNP mutation. Although correlation was detected between the *VvDXS* transcript profile and the accumulation of free monoterpenol odorants, the modulation of *VvDXS* expression during berry development appears to be independent of nucleotide variation in the coding sequence. In order to assess how the non-synonymous mutation may enhance Muscat flavour, an *in vitro* characterization of enzyme isoforms was performed followed by *in vivo* overexpression of each *VvDXS* allele in tobacco. The results showed that the amino acid non-neutral substitution influences the enzyme kinetics by increasing the catalytic efficiency and also dramatically affects monoterpene levels in transgenic lines. These findings confirm a functional effect of the *VvDXS* gene polymorphism and may pave the way for metabolic engineering of terpenoid contents in grapevine.

Key words: Allele expression, DXS, enzyme activity, functional analysis, monoterpenoid profiling, tobacco transformation.

Introduction

Flavour and aroma compounds belong to the large group of secondary metabolites that higher plants produce to mediate necessary interactions with other organisms. These include allelopathic substances (i.e. terpenoid-based resins) or insect attractants which facilitate pollination (Hoballah *et al.*, 2005). Accumulation or secretion of these compounds has to be spatially and/or temporally highly regulated in order for these functions to be carried out. For instance, terpenoid-based resins constitutively accumulate in axial resin canals (Trapp and Croteau, 2001) while insect attractants are emitted from flower petals at the appropriate developmental stage (Chen *et al.*, 2003) and different

aromatic compounds accumulate during fruit ripening to encourage fruit consumption and seed dispersion (Dudareva and Pichersky, 2000).

Aromas in grapevine arise from volatile compounds, such as terpenes, norisoprenoids, and thiols, which are often stored as sugar or amino acid conjugates in the vacuoles of mesocarp cells (Lund and Bohlmann, 2006). It is well known that differences in the relative ratios of volatile compounds and non-volatile precursors present in grape berries greatly influence the varietal 'character' of the wine (Dunlevy *et al.*, 2009; Ebeler and Thorngate, 2009). Factors such as environmental conditions and nutrient availability also affect grape berry composition so that the same grapevine genotype grown in different geographical locations may produce wines with different organoleptic properties (Heymann and Noble, 1987).

Muscat grapes are sweet and fruity, with a rich, musky aroma linked to the presence of the monoterpenes geraniol, linalool, nerol, and α-terpineol, which have low olfactory perception thresholds (Mateo and Jiménez, 2000). Moderate concentrations of monoterpenes can also be found in aromatic non-Muscat varieties such as Gewürztraminer and Riesling (Wilson *et al.*, 1984). On the other hand, monoterpenes are either not detected or present only in trace amounts in more neutral cultivars such as Sauvignon Blanc, Cabernet Sauvignon, Cabernet Franc, Chardonnay, Merlot, and Syrah. Varietal flavour in these cultivars depends on different substances such as methoxypyrazines, C_{13}-norisoprenoids, and volatile sulphur compounds (Strauss *et al.*, 1987).

In plants, all isoprenoids are formed by the conversion of geranyl diphosphate (GPP) that in turn originates from the condensation of two precursors: isopentenyl pyrophosphate (IPP) and its allylic isomer, dimethylallyl pyrophospate (DMAPP). Biosynthesis of IPP and DMAPP occurs through two distinct and partially independent routes, the cytoplasmatic mevalonic acid (MVA) pathway and the plastidial methyl-erythritol-phosphate (MEP) pathway. In grapevine, Luan and Wust (2002) demonstrated that MEP is the dominant route for monoterpene biosynthesis in both leaves and berries. Quantitative genetic analysis recently indicated a structural gene of this pathway, a *Vitis vinifera* 1-deoxy-D-xylulose 5-phosphate synthase (*VvDXS*) gene, as being a positional candidate gene for the concentration of volatile and non-volatile forms of geraniol, nerol, and linalool in berries (Battilana *et al.*, 2009; Duchêne, 2009). Examining nucleotide diversity and linkage disequilibrium within the *VvDXS* gene in grapevines with different genetic backgrounds, and testing for association between individual polymorphisms and Muscat flavour, Emanuelli *et al.* (2010) identified a few significant single nucleotide polymorphisms (SNPs) and a unique haplogroup specific to Muscat varieties. This haplogroup represents a large number of haplotypes with a narrow genetic variability sharing an SNP responsible for the substitution of a lysine with an asparagine at position 284 of the VvDXS amino acid sequence.

In the present study, the nucleotide differences between *VvDXS* haplogroups 284N and 284K were investigated by analysing the full-open reading frame (ORF) cDNA alleles expressed in Moscato Bianco berries. Indeed Moscato Bianco, like most of the Muscat-flavoured genotypes, is heterozygous at the *VvDXS* locus, thus containing a 'Muscat-type' allele (284N) and a 'neutral' allele (284K) as well (Emanuelli *et al.*, 2010). In order to assess how the 284N haplotype may enhance Muscat flavour in grapevine, an integrated study that combines expression profiles—at both the gene and the allele level—in relation to monoterpenoid accumulation with an *in vitro* enzymatic characterization of either protein isoform was performed. In addition, an *in vivo* evaluation of the *VvDXS* allelic difference was carried out by analysing the biosynthesis of monoterpenoids in transgenic tobacco. Putative scenarios regarding how the K284N substitution may affect VvDXS enzymatic kinetics are also discussed by interpreting the results of three-dimensional protein modelling.

Materials and methods

Plant materials and sampling method

Berries of the cultivar Moscato Bianco *V. vinifera* L. kept in the experimental fields of the Fondazione Edmund Mach in San Michele all'Adige (Italy) were sampled at 1–2 week intervals from pre-véraison to 'over-ripe' stages, for a total of 10 collection dates. Grape clusters were picked randomly from 10 plants located in 10 different rows, which contained ~250 plants. Care was taken to collect bunches from different positions on each vine and these were then pooled in order to minimize the effects of field variables such as soil, light, and temperature. The developmental stage of selected berries of the same diameter was determined by monitoring total soluble solids and titratable acidity. Juice samples (80 ml) from berries harvested 7–17 weeks after bloom were measured with FTIR (Fourier transform infrared) using a FOSS instrument (FOSS NIRSystems, Oatley, Australia) for standard maturity analyses. Thus, total soluble solids (°Brix), titratable acidity, pH, and malic and tartaric acid concentrations ($g\,l^{-1}$) were assayed. An aliquot of 200 g of berries from each sample was stored at –20 °C for monoterpenoid analysis, while a subset of berries was frozen in liquid nitrogen and stored at –80 °C pending RNA extraction.

Monoterpenoids analysis

Aroma-active components were extracted and fractionated using solid phase extraction (SPE) and selective retention of either form on a hydrophobic cross-linked polystyrene co-polymer (XAD-2 resin). Both free and bound monoterpenes were identified as described by Gunata *et al.* (1985) and Versini *et al.* (1993) and quantified by high-resolution gas chromatography–mass spectrometetry (HRGC-MS; see Supplementary method 1 available at *JXB* online)

Transcription analysis of the VvDXS *gene in Moscato Bianco*

Total RNA was extracted from pericarp tissue in triplicate for each sample using a SIGMA Spectrum™ Plant Total RNA Kit (Sigma, St Louis, MO, USA). RNA concentrations and 260/280 nm ratios were determined before and after DNase I digestion (Invitrogen, Carlsbad, CA, USA) with a spectrophotometer, and RNA integrity was checked by electrophoresis. First-strand cDNA was synthesized using Superscript™ III Reverse Transcriptase (Invitrogen) according to the manufacturer's instructions. Reaction mixes were prepared using a LightCycler® 480 SYBR Green I Master Mix (Roche, Mannheim, Germany), 2 µl of cDNA

(equivalent to ~10 ng of template) and 0.5 μM of each primer in a final volume of 20 μl.

A combination of several housekeeping genes was used with *geNorm* software to verify the experimental results, while glyceraldehyde 3-phosphate dehydrogenase (*GAPDH*) and elongation factor 1-α (*EF1-α*) (Reid *et al.*, 2006) were selected for determining the normalization factor for each cDNA. Reaction plates included a non-template negative control and both reference and target genes. PCR cycling conditions were: pre-incubation at 95 °C for 5 min, amplification over 40 cycles at: 95 °C for 10 s, 60 °C for 30 s, and 72 °C for 10 s. Finally, a post-PCR melt curve analysis was conducted to detect non-specific amplification in cDNA samples. Real-time reverse transcription-PCR (RT-PCR) efficiencies were calculated from the slope given by LightCycler software (Roche). The second derivative maximum method was used to determine the fractional cycle number referred to as the crossing point (Cp). Expression levels were determined for triplicate biological replicates using serial dilution standard curves for each gene. Primer sequences are reported in Supplementary Table S1 at *JXB* online. Statistical analysis was performed using SPSS software and a pair-wise fixed reallocation randomization test (Pfaffl *et al.*, 2002).

Quantification of allelic pattern using FRET hybridization probes

Full-ORF *VvDXS* cDNA was retrotranscribed, amplified, cloned, and sequenced as described by Emanuelli *et al.* (2010). The alleles of Moscato Bianco differ by three amino acid substitutions (H11Y, K284N, and V560I) in the predicted protein sequence (Supplementary Fig. S1 at *JXB* online). Since only the mutation K284N has been statistically associated with Muscat flavour and it clearly separates the Muscat-type haplogrup N284 from the neutral haplogroups K284, the alleles were renamed in this study as *VvDXS N284* and *VvDXS K284*, respectively. Primers and FRET (fluorescence resonance energy transfer) hybridization probes used in real-time PCRs (Supplementary Table S2) were designed according to the manufacturer's instructions (LightCycler Probe Design Software 2.0, Roche, Applied Science) in order to identify the SNP 1822 (G/T) that causes the K284N amino acid substitution.

The anchor probe was located near the SNP site and was labelled at its 3′ end with fluorescein. An adjacent sensor probe was placed one nucleotide apart from the anchor probe and was labelled with Red 640 at its 5′ end. The sensor probe was designed to be perfectly aligned with *VvDXS K284*. FRET probe synthesis was performed by TIB MOLBIOL (Berlin, Germany).

cDNA melting curve analysis

Prior to using the FRET hybridization probes, real-time RT-PCRs were carried out using a LightCycler®480SYBER Green I Master Mix (Roche) in 20 μl reactions containing cDNA and 0.3 μM of each primer for testing.

The melting curves of different mixtures of pENTR/D-TOPO:VvDXS N284 and pENTR/D-TOPO:VvDXS K284 were first normalized by converting the maximum fluorescence value of each amplicon to 1 and the minimum fluorescence value to 0, with all other values adjusted proportionally. The fractional values of *VvDXS K284* (γVvDXS K284s) were calculated as the fraction of pENTR/D-TOPO:VvDXS K284 in the two-part plasmid mixture at a given temperature. Observed γVvDXS K284s(Ob) values were then calculated as described in Jeong *et al.* (2007) by comparing every temperature pair in which <90% but >10% of *VvDXS* amplicons were still double-stranded. γVvDXS K284(Ob) values of each mixture were then corrected for probe bias. Because the sensor FRET probe matches perfectly with *VvDXS K284* but has a 1 bp mismatch with *VvDXS N284*, the γVvDXS K284s(Ob) might incorrectly overstate γVvDXS K284s. These γVvDXS K284s(Ob) values were therefore subsequently corrected using the fraction value of the 1:1 (5:5) molar mixture to yield the bias-corrected fraction value, γVvDXS K284s(c). The melting curves of Moscato Bianco cDNA samples were analysed as described for the plasmid mixtures. Fraction values and standard deviations are reported in Supplementary Table S3 at *JXB* online.

VvDXS enzyme characterization and in vitro *assay*

The full-ORF *VvDXS* was amplified using the forward primer (5′-TTGGATCCGGGGTTTGTGCATCACTTTCG-3′) and the reverse primer (5′-TTTCTCGAGCTATGACATGATCTCCAG-GGC-3′), which contain non-hybridizing *Bam*HI and *Xho*I sites, respectively.

The amplified fragment, without the putative chloroplast signal target sequence, was cloned into pCR®-Blunt (Invitrogen), and *Escherichia coli* DH5α was employed as the host strain for gene manipulation. The *VvDXS N284* and *VvDXS K284* alleles were identified using *Sac*II restriction enzyme and sequenced in order to determine the authenticity of the cloned fragment.

The alleles were then subcloned into the *Bam*HI and *Xho*I restriction sites of pET30a (KanR and CamR); *E. coli* BL21-DE3 plus pLysS was employed as the host strain for protein synthesis, and 0.8 mM isopropyl-β-D-1-thiogalactopyranoside (IPTG) was used to overexpress the HIS_6-VvDXS protein. SDS–PAGE and immunoblot analyses were carried out to confirm expression of the recombinant protein. SDS–PAGE was performed on an electrophoresis system with 4–20% polyacrylamide gels (NuSep, Sydney, Australia) under denaturing conditions. Proteins from gels were transferred electrophoretically onto a polyvinylidene difluoride (PVDF) membrane. Non-fat dried milk was used as the blocking agent at 5% in phosphate-buffered saline (PBS; 17 mM NaCl, 3 mM KCl, 10 mM Na_2HPO_4, 2 mM KH_2PO_4, pH 7.4). A His·Tag® monoclonal primary antibody (Sigma) and a goat anti-mouse IgG–alkaline phosphatase conjugate (Promega, Madison, WI, USA) secondary antibody were used to detect recombinant HIS_6-VvDXS. Cross-reacting protein bands were visualized with a BCIP/NBT solution (Bio-Rad, Hercules, CA, USA).

Protein purification was carried out using a His GraviTrap prepacked column (GE Healthcare Bio-Sciences, Sydney, Australia). The proteins were eluted with 20–500 mM imidazole at pH 7.4. Protein concentrations were estimated using the Bio-Rad assay kit.

Enzyme assay

Assay reaction mixtures contained 100 mM TRIS-HCl (pH 8.0), 2 mM $MgCl_2$, 2 mM thiamine pyrophosphate (TPP), 2 mM pyruvate, 2 mM DL-glyceraldehyde 3-phosphate (DL-GAP), 2 mM dithiothreitol (DTT), and 5 μg of purified enzyme in a final volume of 100 μl. The mixture was incubated at 37 °C for 40 min, the reaction was terminated by adding 100 μl of acetone, and the denatured protein was removed by centrifugation at 13 000 rpm for 15 min. The supernatant was dried, resuspended in 20 μl of 100 mM KH_2PO_4 (pH 3.0), and 10 μl was used to analyse the reaction product. 1-Deoxy-D-xylulose 5-phosphate (DXP) produced by the enzyme reaction was analysed by HPLC (Agilent 1200 Series) with a Luna 100A NH_2 (4.6 mm×250 mm) column (Phenomenex, Sydney, Australia) eluted with 100 mM KH_2PO_4 (pH 3.0) at a flow rate of 1.0 ml min^{-1}. DXP was detected by its refractive index and eluted at 9 min under these conditions. The amount of DXP produced was estimated precisely using chemically synthesized DXP as the standard (Echelon Biosciences, Salt Lake City, UT, USA).

VvDXS allele activity was determined in the presence of a fixed concentration of the second substrate using a coupled assay method. Different concentrations of pyruvate (0.025–20 mM) with 5 mM DL-GAP, and different concentrations of DL-GAP (0.080–20 mM) with 5 mM pyruvate were used. The IPP inhibition assay was carried out using a mixture containing 100 mM TRIS-HCl (pH 8.0), 2 mM $MgCl_2$, 2 mM TPP, 5 mM pyruvate, 0.625 mM DL-GAP, 2 mM DTT, and 2 μg of purified enzyme in a final

volume of 100 µl. Different concentrations of IPP (0.0062–1.5 mM) were used. The mixtures were incubated at 37 °C for 40 min, and the data were submitted to non-linear regression analysis using SigmaPlot for Windows.

Submission of sequences to 3D structure prediction servers

Putative VvDXS protein sequences were separately submitted to 3D-Jury http://meta.bioinfo.pl, INHUB http://inub.cse.buffalo.edu, Phyre de novo http://www.imperial.ac.uk/phyre/ (Kelley and Sternberg, 2009), the Robetta server http://robetta.bakerlab.org/, and the I-TASSER server http://zhang.bioinformatics.ku.edu/I-TASSER/. The latter was ranked number 1 server in the recent Critical Assessment of Techniques for Protein Structure Prediction (CASP7) competition for homology modelling, and threading. I-TASSER combines threading, *ab initio* modelling, and structural refinement methods to build reliable models (Zhang, 2008). The Eris server http://troll.med.unc.edu/eris/login.php was also used to test the stability in terms of $\Delta\Delta G$ by amino acid substitution (Yin *et al.*, 2007, 2010).

*Tobacco (*Nicotiana tabacum *cv Samsun) transformation*

Gateway technology (Invitrogen) was employed to transfer the cDNA *DXS* alleles subcloned in pENTR/D-TOPO to a pK7WG2 plant expression vector downstream of the cauliflower mosaic virus (CaMV) 35S promoter (Karimi *et al.*, 2002). The final constructs were designated as pK7WG2:VvDXS N284 and pK7WG2:VvDXS K284, and *E. coli* One Shot TOP10 was employed as the host strain for gene manipulation.

The constructs generated in *E. coli* One Shot TOP10 were transformed into *Agrobacterium tumefaciens* EHA 105 (Hood *et al.*, 1993) by electroporation (2 kV, 90 Ω, 25 µF). Tobacco was then transformed with *A. tumefaciens* containing pK7WG2:VvDXS N284 or pK7WG2:VvDXS K284 following a modified Gallois and Marinho (1995) protocol; for more details see Supplementary method 2 at *JXB* online.

Results

Monoterpene accumulation in Moscato Bianco berries correlates with VvDXS *expression*

Berries of Moscato Bianco are known to be rich in linalool, nerol, and geraniol (Strauss *et al.*, 1986; Ebang-Oke *et al.*, 2003), thus these monoterpenes were analysed and quantified throughout berry development to investigate if there is a correlation with *VvDXS* gene expression.

During berry ripening, free and bound forms of monoterpenes accumulated differently, as shown in Fig. 1. Concentrations of the three major monoterpenes followed the same upward trend until 12 weeks after bloom, corresponding to the second week after véraison. Thereafter, the accumulation patterns of the free and bound forms diverged; free forms increased slightly, reaching the maximum level of 899.4 µg kg^{-1} at 14 weeks after bloom (harvest), and then decreased during the over-ripe stage. Bound forms, on the other hand, followed the sugar content trend (Supplementary Fig. S2 at *JXB* online), continuing to increase even when berries were over-ripe (14–17 weeks post-flowering).

A relative quantification of *VvDXS* levels was performed by real-time RT-PCR. The *VvDXS* expression was normalized based on the level of the *EF1-α* and *GADPH* housekeeping genes. Evidence for the modulation of *VvDXS* expression during the ripening stages is provided by a significant increase in expression (P <0.05) at 10, 11, and 12 weeks after bloom (Fig. 1). This is slightly earlier than the peak of accumulation of free linalool, nerol, and geraniol compounds. A Kolmogorov–Smirnov test revealed a positive correlation (P <0.05) for the *VvDXS* expression

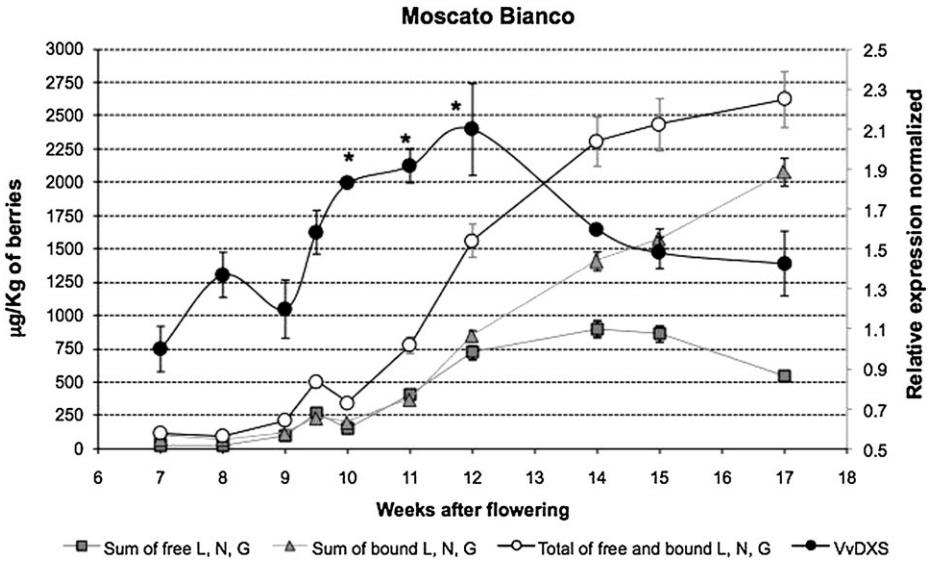

Fig. 1. Transcription profile of *VvDXS* and monoterpene variation during berry ripening in Moscato Bianco. For *VvDXS* expression analysis, data were calculated as gene expression relative to the expression of the housekeeping genes *EF1-α* and *GAPDH* (filled circles). Data are shown as means ±SDs of triplicate experiments and normalized to the first sampling point. Significant changes in the transcript abundance are indicated by * (P <0.05). The contents of the monoterpenes linalool (L), nerol (N), and geraniol (G) (µg kg^{-1} of berries) at each sampling time are reported for free forms, bound forms, and the sum of free and bound forms.

profile and accumulation of free monoterpenoids in this cultivar.

Using normalized data and a calculation of a cumulative sum (CuSum) procedure, combined with a Jonckheere–Terpstra trend test and χ^2 test, two *VvDXS* trend point changes during berry development were identified. The first trend change occurred at 9 weeks post-flowering (P <0.05) and a second change point (P <0.05) was observed at 12 weeks after flowering (Fig. 1).

The expression behaviour of Moscato Bianco *VvDXS* alleles was investigated by quantitative real-time RT-PCRs using FRET hybridization probes specifically designed for the *VvDXS* allelic variants. Melting curve analysis distinguished plasmid mixtures with different pENTR/D-TOPO:VvDXS N284 and pENTR/D-TOPO: VvDXS K284 molar ratios (Supplementary Table S3 at *JXB* online) and, therefore, allelic expression levels could be compared.

VvDXS N284 and *VvDXS K284* alleles displayed nearly equal expression (ratio of 1.5) and this result was consistent throughout the developmental stages of the grape berries. Moreover, a preferential allelic expression was not identified even in the stages where statistically significant up-regulation of *VvDXS* gene expression was found (Fig. 1).

VvDXS N284 has greater catalytic efficiency than the VvDXS K284 enzyme form

The enzymatic activity of VvDXS N284 and VvDXS K284 was investigated with the aim of elucidating the consequences of the K284N non-neutral substitution on catalytic efficiency. A significant protein level was obtained by inducing recombinant protein production with 0.8 mM IPTG at 28 °C for 3 h, and eluting the HIS_6-tagged protein from Ni-NTA columns using 200 mM imidazole. Purified recombinant DXS was present as a single band on an SDS–polyacrylamide gel with a molecular mass of ~77 kDa (Supplementary Fig. S3 at *JXB* online).

The effect of temperature on enzyme activity was investigated over a range of 25–50 °C. Maximum activity was observed at 37 °C and the pH optimum in sodium citrate buffer was 8.0. Other parameters, such as the incubation time required to ensure reactions occurred within the linear range, were determined for each allele before assessment of the kinetic parameters.

Michaelis–Menten constants for pyruvate and DL-GAP were determined by fitting hyperbolic plots of initial velocities versus substrate concentrations (Fig. 2). Initial velocities were calculated from the slope of the product (DXP) versus time plots at each substrate concentration. Hyperbolic regression results showed that VvDXS N284 and VvDXS K284 had values of $K_m^{pyruvate}$=585.2±86.8 μM and $K_m^{pyruvate}$=661.2±80.1 μM, respectively, and followed Michaelis–Menten-type kinetics. However, DL-GAP did not exhibit typical hyperbolic saturation type kinetics (Supplementary Fig. S4 at *JXB* online), and biochemical properties were calculated by fitting an amount of DXP on a substrate inhibition kinetic curve. VvDXS N284 yielded K_m^{GAP}=1.67±0.62 mM and V_{max}=133.6±17.2 μmol min^{-1} mg^{-1} of protein, while VvDXS K284 yielded K_m^{GAP}=1.78±0.57 mM and V_{max}=76.0±8.6 μmol min^{-1} mg^{-1} of protein.

The catalytic efficiency k_{cat}/K_m for VvDXS N284 was calculated at 2.1×10^5 M^{-1} s^{-1}, while the k_{cat}/K_m value for VvDXS K284 was 1.1×10^5 M^{-1} s^{-1}. Thus, the catalytic efficiency of VvDXS K284 was lower than that of VvDXS N284 by a factor of ~2.

Three-dimensional protein modelling and amino acid substitution at position 284

A complete three-dimensional protein structure of VvDXS N284 and VvDXS K284 was obtained by I-TASSER for deciphering the possible effects of K284N change on the structural conformation of VvDXS. Two segments were reconstructed by *ab initio* modelling using the crystallized structure (2O1×A) of *Deinococcus radiodurans* DXS as template, which gave 48% sequence similarity with VvDXS (Supplementary Fig. S5 at *JXB* online). A structural TM-score of 0.80, representing the value of the alignment between the model and the PDB structures, and coverage of 0.81, representing the number of structurally aligned residues divided by the length of the model, were found for the VvDXS model (Fig. 3A).

When the two VvDXS forms were compared, the lysine to asparagine substitution at site 284 was positioned in an α-helix segment and gave rise to a change in the calculated electrostatic potential surface that appeared on the fourth and fifth β-sheet linker junction of domain I (Fig. 3B). Protein stability was then calculated using the Eris server, which predicted a stabilizing change of $\Delta\Delta G$= –9.44 kcal mol^{-1} for the K284N amino acid substitution.

Overexpression of VvDXS N284 *and* VvDXS K284 *alleles differentially affects the monoterpenes production in transgenic tobacco*

T_0 transgenic tobacco plants were generated with either the *VvDXS N284* allele (B3 lines) or the *VvDXS K284* allele (B6 lines) under control of the CaMV 35S promoter. T-DNA copy number, evaluated by Southern analysis with an *nptII* gene fragment as a probe, ranged from 1 to 4 (Supplementary Fig. S6A, B at *JXB* online). All transgenic lines, including the single-copy (B3-2 and B6-13) and the multiple-copy transgenic lines (B3-12 and B6-14) for each allele, were analysed for their secondary metabolites content. The amounts of volatile and glycosidically bound terpenoid compounds found in these plants are reported in Fig. 4 and in Supplementary Tables S4 and S5 at *JXB* online. B3-2 and B3-12 lines contained high levels of free geraniol and geranic acid which were not detected in wild-type plants or in the B6-13 line. The presence of glycosidically bound aromatic compounds was assessed after the enzymatic hydrolysis of glycoside extracts. HRGC-MS analysis of liberated volatile compounds showed that wild-type plants contained the same compounds detected in transformed

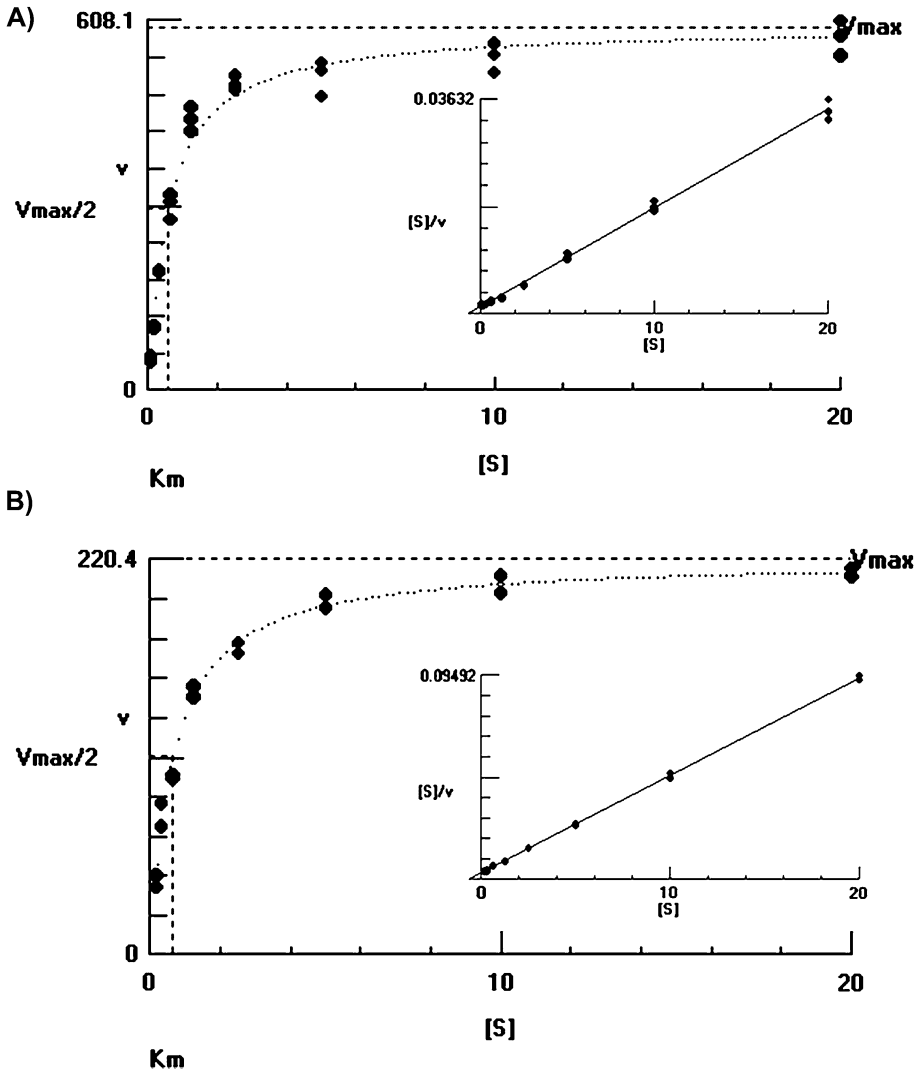

Fig. 2. Michaelis–Menten constants of VvDXS_N284 (A) and VvDXS_K284 (B) isoforms for pyruvate determined by fitting hyperbolic plots of initial velocities (v) versus substrate [S] concentration (mM). Initial velocities are calculated from the slope of the product (DXP) versus time plots at each substrate concentration. Hyperbolic regression results showed that VvDXS N284 and VvDXS K284 had values of K_m=585.2±86.8 μM and K_m=661.2±80.1 μM, respectively. The Hanes–Woolf plot graphs inside show a linear representation of these results.

plants but at different concentrations. Bound forms of monoterpenoids were present at low levels in the wild type, with geraniol and its derivative geranic acid being the most abundant. Bound monoterpene concentrations increased in transformed lines, with a higher accumulation in the B3-2 and B3-12 lines in comparison with the B6-13 and B6-14 lines. B3-12 accumulated 100-fold more geraniol than the wild-type plants, whereas in B6-14, geraniol was 4-fold higher than in wild-type plants. When comparing the single-copy transformed plants (B3-2 versus B6-13), geraniol was 20-fold higher in the line transformed with the *VvDXS N284* allele (B3-2) than in the line transformed with the *VvDXS K284* allele (B6-13).

Nor-isoprenoids, benzenoids, and fatty acid derivatives were also detected in higher levels in transformed plants compared with the control plants, but no significant differences were found between the B3 and B6 transformed lines (Supplementary Tables S4, S5 at *JXB* online).

Discussion

The major purpose of the present study was to assign a functional validation of the missense mutation that has been associated with Muscat-flavoured grapevines (Emanuelli *et al.*, 2010) and which causes a K284N substitution in the grapevine VvDXS enzyme. The connection between *VvDXS* gene expression and the monoterpenoid accumulation pattern was extensively investigated during grape berry development, as were the biochemical properties of the enzymes encoded by the different *VvDXS* alleles.

Monoterpenoid formation and VvDXS *expression in a Muscat-type cultivar*

Two distinct accumulation trends for free and bound monoterpenes during berry development in Moscato Bianco were observed in this study. Up to 2 weeks after veraison,

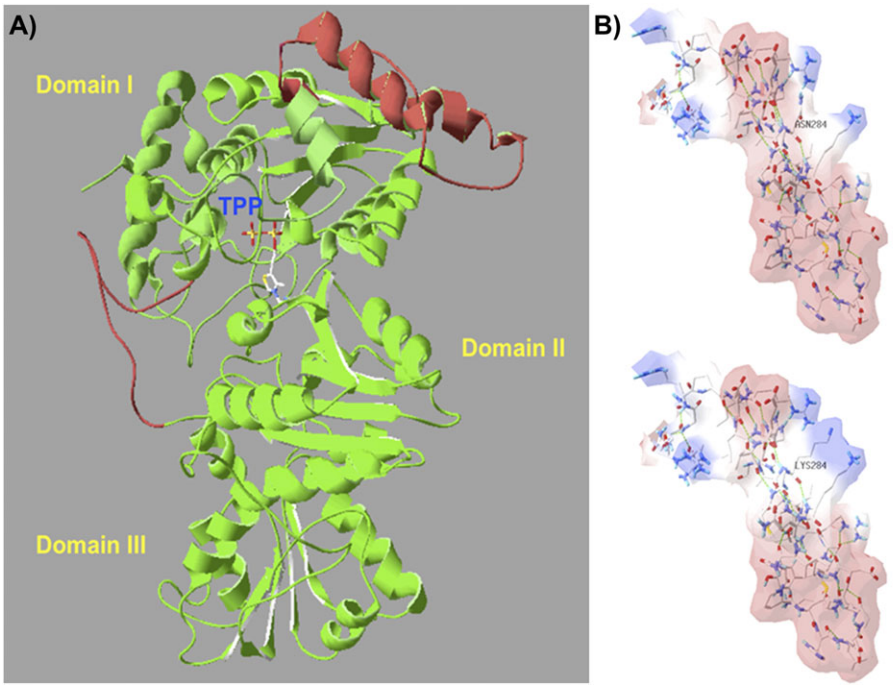

Fig. 3. Three-dimensional VvDXS protein modelling and the putative electrostatic change conferred by the N–K substitution. DXS protein is a dimer and the structure of its monomers can be divided into three domains (I, II, and III). The active site is located between domain I and II, and the thiamine pyrophosphate coenzyme (TPP) is placed on the interface and interacts on domain II as described by Xiang *et al.* (2007). (A) The complete three-dimensional model of VvDXS obtained by the I-TASSER server. Two segments were reconstructed by *ab initio* modelling using the DXS crystallized structure (2O1×A) of *Deinococcus radiodurans* as template. Red parts represent linkers modelled, and mutation K284N falls within an α-helix of 46 amino acids in a linker between β-sheet 4 and 5 of domain I. (B) Electrostatic potential surface of the two VvDXS allelic forms calculated by SPDBV 4.01. Red and blue surfaces indicate the negative and positive potential, respectively.

free and bound monoterpenoids were present at low levels and correlate well. In the later stages of berry ripening, free and glycosidically bound forms showed a different accumulation pattern (Fig. 1). A general increase in monoterpenoids was indeed observed after this developmental stage, but, while volatile monoterpenes showed a small rise in parallel with sugar accumulation, bound forms exhibited a substantial increase in concentration during this time. These results show how the distribution of monoterpenoids in the grape berry changes during ripening and they are consistent with previous findings reported for Muscat grapes, in particular for Muscat de Frontignan (Ebang-Oke el al., 2003) and other Muscat varieties (Strauss *et al.*, 1986).

Since monoterpenoids exhibited an accumulation profile suggesting that they are regulated during berry development, *VvDXS* expression was studied in relation to monoterpenes biosynthesis. The results highlighted a significant correlation between *VvDXS* expression and the accumulation profile of monoterpenes, especially with the volatile compounds linalool, geraniol, and nerol. The stages where a significant upward trend was detected for *VvDXS* expression showed a rapid rise in monoterpenoid accumulation for both bound and free forms.

Volatile monoterpene biosynthesis and *VvDXS* expression declined during later fruit ripening, while bound forms kept increasing even in over-ripe berries. Biosynthesis of bound monoterpenes is thought to be influenced by the non-specific activity of glycosyl transferases (Wilson *et al.*, 1986). A consequence of the glycosylation is an extensive redistribution of the grape aroma compounds into flavourless, conjugated forms throughout the berry, and this could weaken any direct correlation between *VvDXS* expression in berry skins and the total content of bound monoterpenoids.

These results shows that there is a temporal regulation of *VvDXS* transcription during berry development, despite *DXS* predominantly playing a housekeeping role in other plant systems (Kim *et al.*, 2005). In fact, *DXS* expression was reported to be tightly regulated in maize where *ZmDXS* is highly expressed in photosynthetic tissues during early seedling development (Cordoba *et al.*, 2011). In *Arabidopsis* and rice, the transcription profile of *DXS* is altered by factors such as light (Botella-Pavia *et al.*, 2004; Kim *et al.*, 2005), and a high isoprenoid demand also enhances *DXS* transcription (Enfissi *et al.*, 2005). Concordantly, the data presented here corroborate the idea that the modulation of this structural gene could also follow isoprenoid demand in grape berries.

Allelic expression pattern of VvDXS *during berry development*

The non-neutral K284N substitution is found in almost all Muscat varieties, suggesting that the causal 'gain-of-function' mutation was selected by intense breeding practices (Emanuelli *et al.*, 2010).

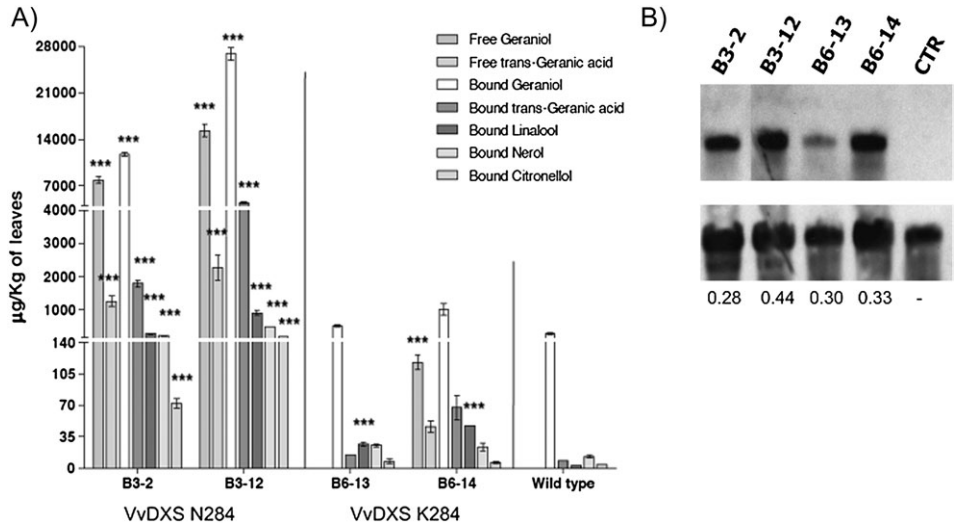

Fig. 4. Monoterpenoid accumulation in transgenic tobacco plants overexpressing VvDXS N284 and VvDXS K284. Volatile and glycosidic monoterpenoid forms were isolated by solid-phase extraction and quantified by HRGC-MS analysis as described in the Materials and methods. Data are shown as means ±SDs of triplicate experiments. (A) B3-2 and B6-13 lines present a single copy of the transgene, whereas B3-12 and B6-14 lines present multicopy transgene insertion. Significant differences in monoterpenoid accumulation in transformed lines compared with wild-type plants are indicated as ***P <0.01 (two-way analysis of variance). (B**)** Northern blot results. B3-2 and B6-13 lines show similar expression levels; values are the ratio of band density (*VvDXS*/*18S*) calculated by using ImageJ software. CTR, wild-type line.

In order to delve deeper into *VvDXS* transcriptional regulation, the expression pattern of both Moscato Bianco *VvDXS* alleles during berry development was determined. *VvDXS N284* was expressed to a slightly greater extent than *VvDXS K284* during the entire ripening curve, but with no significant variation of the expression ratio among the sampling points. Apparently both alleles are equally up-regulated even when the change in *VvDXS* transcript accumulation is significant. Therefore, the modulation observed for *VvDXS* expression during berry development seems to be independent of the nucleotide variation in the coding sequence. This result would suggest the involvement of other factors influencing *VvDXS* expression dynamics, which could be related to quantitative trait loci (QTLs) having minor effects on Muscat flavour detected in previous mapping experiments (Doligez *et al.*, 2006; Battilana *et al.*, 2009; Duchêne *et al.*, 2009).

Enzyme kinetics and three-dimensional modelling

Enzymatic proprieties of proteins encoded by the VvDXS alleles: Kinetic analyses showed that the substrate affinities of the proteins encoded by the *VvDXS* alleles are similar in terms of $K_m^{Pyruvate}$ and K_m^{GAP}, but a major difference was found in the catalytic efficiencies of the enzymes (k_{cat}/K_m), VvDXS N284 being twice as efficient as VvDXS K284. VvDXS efficiency was 10 times lower than that of the the DXS of *E. coli* (Kuzuyama *et al.*, 2000), but it was greater than other DXS characterized in bacteria (Hahn *et al.*, 2001; Bailey *et al.*, 2002).

The effect of increasing concentrations of substrates (pyruvate and DL-GAP) on VvDXS activity was evaluated in the *in vitro* assays, and a common result was observed for the two isoforms. As soon as DL-GAP reached saturation level, it led to inhibition of the reaction (Supplementary Fig. S4 at *JXB* online), which is in agreement with the behaviour observed for DXS in *Rhodobacter capsulatus* (Hahn *et al.*, 2001). On the other hand pyruvate concentrations did not affect VvDXS activity.

While saturating levels of DL-GAP might not occur in an *in vivo* situation, it suggests a possible point of regulation of this enzyme (Hahn *et al.*, 2001). The effect of IPP accumulation on VvDXS activity was also investigated since a possible negative feedback regulation has been suggested. Indeed, Guevara-Garcìa *et al.* (2005) found that by reducing IPP/DMAPP accumulation (in the presence of fosmidomycin), the DXS protein consistently accumulated to higher levels, while no other significant differences were observed for any other proteins in the MEP pathway. The experiments conducted here show that IPP accumulation does not affect the *in vitro* VvDXS activity, thus circumscribing IPP feedback regulation to protein accumulation if this regulation does exist in grape berries.

DXS and other genes of the MEP pathway have been previously shown to be regulated at the post-transcriptional level. In particular, post-transcriptional regulation of *DXS* could be triggered by key enzymes downstream of the pathway; for example, *phytoene synthase* (*PSY*) has been shown to control metabolic flux to the carotenoid pathway (Rodrìguez-Villalòn *et al.*, 2009) and environmental changes (Laule *et al.*, 2003; Wolfertz *et al.*, 2004; Guevara-García *et al.*, 2005; Sauret-Güeto *et al.*, 2006). A multilevel tight regulation of DXS activity seems to be a crucial point of control of this pathway in plants, as *DXS*, besides affecting chlorophyll content (Mandel el al., 1996), also plays an essential role in chloroplast development during leaf cell maturation (Araki *et al.*, 2000; Flores-Pérez *et al.*, 2008).

Three-dimensional protein modelling and altered enzyme properties

Due to the crucial role the DXS protein plays in certain organisms, it has been studied in bacteria and in plants (Mandel *et al.*, 1996; Estévez *et al.*, 2001) and its sequence is highly conserved. DXS proteins also display weak sequence homology with transketolases (TKs) (Bouvier *et al.*, 1998; Querol *et al.*, 2001). TK and DXS catalyse similar biochemical reactions, and they all require the coenzyme TPP (Lois *et al.*, 1998; Sprenger *et al.*, 1997).

To date, there is no empirically determined plant DXS three-dimensional structure available on which to model the grapevine homologue of DXS and predict the possible consequences of the amino acid changes on protein structure. However, a few significant bacterial templates suitable for modelling have been identified by alignment searches. DXS protein is a dimer, and the structure of its monomers can be divided into three domains each of which is homologous to its equivalent domains in TK. The arrangement of these domains is different to that of TK, resulting in a different dimer organization (Xiang *et al.*, 2007).

A linker located near the active site, between the fourth and fifth β-strands of domain I, corresponds to residues 267–312 of VvDXS. Modification in this region may reasonably affect the activity of the protein, thus altering the conformation or the thermodynamic stability ($\Delta\Delta G$) of the dimer. However, information on the physiological role of a possible change on the protein structure must await further investigation.

Overexpression of VvDXS *in tobacco resulted in a significant increase in monoterpene production*

The DXS enzyme catalyses a limiting step in IPP biosynthesis and it has been shown to play a regulatory role in isoprenoid biosynthesis. DXS overexpression has up to now been evaluated in several different plant systems. Estévez *et al.* (2000) reported increased accumulation of several plastidic isoprenoids in transgenic *Arabidopsis* lines overexpressing *DXS*. Moreover, a positive correlation between the amount of *DXS* transcript and the production of specific isoprenoids has been found in several other plant systems. However, its impact on the production of secondary metabolites has not always been confirmed. Transgenic tomato expressing a bacterial *DXS* gene under a fruit-specific promoter confirmed that *DXS* up-regulation correlated with a higher accumulation of carotenoids and chlorophylls, while *DXS* overexpression in transgenic tomato driven by the CaMV 35S promoter did not result in an increase in these compounds (Enfissi *et al.*, 2005). *DXS* overexpression in the aromatic plant spike lavender (Munoz-Bertomeu *et al.*, 2006) resulted in an elevated level of essential oil production. Monoterpenoids such as linalool and α/β- pinene are common compounds of essential oils, and production of these increased in transgenic spike lavender by up to double that of the wild type.

Induction of higher levels of isoprenoids by stable *VvDXS* overexpression in a heterologous plant system enabled the assessment of the major role of *VvDXS* in monoterpene biosynthesis. Monoterpenoid profiles of both free and glycosidically bound forms are clearly different between the transgenic and non-transformed lines (Fig. 4).

Volatile monoterpenoids were not found in the wild-type lines, where only glycosylated geraniol was detected in notable amounts. Free geraniol and geranic acid accumulated at high levels in plants overexpressing the *VvDXS N284* allele (B3 lines) and in trace amounts in the multicopy line of *VvDXS K284* (B6-14 line).

The differences suggest that glycosidase and glycosyltransferase enzymes in tobacco might play a role in the emission of monoterpenoids. In other plant systems (Lewinsohn *et al.*, 2001; Lücker *et al.*, 2001; Aharoni *et al.*, 2003) overexpression of a terpene synthase induced the accumulation of free and glycosylated monoterpenoids at different ratios, suggesting that the genetic background of transgenic plants affects the induction of monoterpenoid metabolism. Nevertheless the major monoterpenoid compounds found in the leaves and berries of Muscat-flavoured grapevines (i.e. geraniol, geranic acid, linaool, nerol, and citronellol; Wilson *et al.*, 1984) were actually detected in tobacco lines expressing *VvDXS*. Moreover the two alleles of *VvDXS* showed strong differential effects on monoterpenoid production when overexpressed in tobacco. Indeed, a dramatic increase in glycosylated monoterpenes was found in plants overexpressing the *VvDXS N284* allele (B3 lines), up to 20 times more than the level seen when *VvDXS K284* (B6 lines) was overexpressed.

The finding that *VvDXS N284* encodes an enzyme with greater catalytic efficiency than that encoded by *VvDXS K284* is supported by the *in vivo* experiments in transgenic tobacco plants. These results extend the previous work that linked this *DXS* gene to monoterpenoid production and Muscat flavour in grapevine, and provide new insights and a structural framework for further experiments aimed at understanding the structure and dynamics of this key enzyme which influences the aromatic phenotype of grapevine cultivars.

Supplementary data

Supplementary data are available at JXB online

Supplementary method 1. Monoterpenoid analysis: preparation of volatile extracts from grape berries and tobacco leaves

Supplementary method 2. Tobacco transformation procedure.

Figure S1. Alignment of VvDXS isoforms and the non-synonymous mutations found in Moscato Bianco.

Figure S2. Evolution of sugar and monoterpenoid contents during berry maturation of grapevine muscat cultivar.

Figure S3. His-tagged protein purification using Ni-NTA resin and immunoblot test.

Figure S4. Effects of substrate concentration on the activities of purified VvDXS N284 and VvDXS K284.

Figure S5. Sequence comparison of the predicted amino acid sequences of DXS and secondarty structure.

Figure S6. Digested transgene PCR products of transformed T_0 tobacco plants and Southern blot.

Table S1. List of primers used in the real-time RT-PCR analysis

Table S2. List of primers and FRET hybridization probes used in real-time PCR and melting curve analysis.

Table S3. Normalized DNA melting curves used to calculate the fractional value of each allele in plasmid mixtures of pENTR/D-TOPO:VvDXS N284 pENTR/D-TOPO:VvDXS K284 with different molar ratios.

Table S4. Concentration (μg kg^{-1} of leaves, dry weight) of free aromatic compounds from T_0 tobacco plants transformed with *VvDXS N284* and *VvDXS K284* alleles.

Table S5. Concentration (μg kg^{-1} of leaves, dry weight) of bound aromatic compounds from T_0 tobacco plants transformed with *VvDXS N284* and *VvDXS K284* alleles.

Acknowledgements

We are grateful to Mario Malacarne and Emanuela Betta for technical assistance and to Alessandro Cestaro for bioinformatic support. We would like to thank Sue Maffei of CSIRO Plant Industry (Adelaide) for the HPLC analysis and valuable discussions. This research was partly funded by a Short Term Scientific Mission grant awarded to JB by COST Action 858 Viticulture.

References

Aharoni A, Giri A, Deuerlein S, Griepink F, de Kogel W, Verstappen F, Verhoeven H, Jongsma M, Schwab W, Bouwmeester H. 2003. Terpenoid metabolism in wild-type and transgenic Arabidopsis plants. *The Plant Cell* **15,** 2866–2884.

Araki N, Kusumi K, Masamoto K, Niwa Y, Iba K. 2000. Temperature-sensitive Arabidopsis mutant defective in 1-deoxy-d-xylulose 5-phosphate synthase within the plastid non-mevalonate pathway of isoprenoid biosynthesis. *Physiologia Plantarum* **108,** 19–24.

Bailey AM, Mahapatra S, Brennan PJ, Crick DC. 2002. Identification, cloning, purification, and enzymatic characterization of Mycobacterium tuberculosis 1-deoxy-d-xylulose 5-phosphate synthase. *Glycobiology* **12,** 813–820.

Battilana J, Costantini L, Emanuelli F, Sevini F, Segala C, Moser S, Velasco R, Versini G, Grando MS. 2009. The 1-deoxy-d-xylulose 5-phosphate synthase gene co-localizes with a major QTL affecting monoterpene content in grapevine. *Theoretical and Applied Genetics* **118,** 653–669.

Botella-Pavía P, Besumbes O, Phillips MA, Carretero-Paulet L, Boronat A, Rodríguez-Concepción M. 2004. Regulation of carotenoid biosynthesis in plants: evidence for a key role of hydroxymethylbutenyl diphosphate reductase in controlling the supply of plastidial isoprenoid precursors. *The Plant Journal* **40,** 188–199.

Bouvier F, d'Harlingue A, Suire C, Backhaus RA, Camara B. 1998. Dedicated roles of plastid transketolases during the early onset of isoprenoid biogenesis in pepper fruits. *Plant Physiology* **117,** 1423–1431.

Chen F, Tholl D, D'Auria JC, Farooq A, Pichersky E, Gershenzon J. 2003. Biosynthesis and emission of terpenoid volatiles from Arabidopsis flowers. *The Plant Cell* **15,** 481–494.

Cordoba E, Porta H, Arroyo A, San Romàn C, Medina L, Rodrìguez-Concepciòn M, Leòn P. 2011. Functional characterization of the three genes encoding 1-deoxy-d-xylulose 5-phosphate synthase in maize. *Journal of Experimental Botany* **62,** 1–16.

Doligez A, Audiot E, Baumes R, This P. 2006. QTLs for muscat flavor and monoterpenic odorant content in grapevine *Vitis vinifera* L. *Molecular Breeding* **18,** 109–125.

Duchêne E, Butterlin G, Claudel P, Dumas V, Jaegli N, Merdinoglu D. 2009. A grapevine (*Vitis vinifera* L.) deoxy-d-xylulose synthase gene colocates with a major quantitative trait loci for terpenol content. *Theoretical and Applied Genetics* **118,** 541–552.

Dudareva N, Pichersky E. 2000. Biochemical and molecular genetic aspects of floral scents. *Plant Physiology* **122,** 627–633.

Dunlevy J, Kalua C, Keyzers R. 2009. The production of flavour and aroma compounds in grape berries. In: Roubelakis-Angelakis KA, ed. *Grapevine molecular physiology & biotechnology*, 2nd edn. Dordrecht: Springer, 293–340.

Ebang-Oke JP, de Billerbeck GM, Ambid C. 2003. Temporal expression of the Lis gene from *Vitis vinifera* L., cv.Muscat de Frontignan. In: Le Quere JL, Etiećvant PX, eds. *Flavour research at the dawn of the twenty-first century. Proceedings of the 10th Weurman Flavour Research Symposium*, Beaune, France, 25–28 June, 2002. Paris: Editions Lavoisier, 321–325.

Ebeler SE, Thorngate JH. 2009. Wine chemistry and flavor: looking into the crystal glass. *Journal of Agricultural and Food Chemistry* **57,** 8098–8108.

Emanuelli F, Battilana J, Costantini L, Le Cunff L, This P, Grando MS. 2010. A candidate gene association study for muscat flavor in grapevine *Vitis vinifera* L. *BMC Plant Biology* **10,** 241.

Enfissi E, Fraser P, Lois L, Boronat A, Schuch W, Bramley P. 2005. Metabolic engineering of the mevalonate and non-mevalonate isopentenyl diphosphate-forming pathways for the production of health-promoting isoprenoids in tomato. *Plant Biotechnology Journal* **3,** 17–27.

Estévez JM, Cantero A, Romero C, Kawaide H, Jimenez L, Kuzuyama T, Seto H, Kamiya Y, Leon P. 2000. Analysis of the expression of *CLA1*, a gene that encodes the 1-deoxyxylulose 5-phosphate synthase of the 2-C-methyl-d-erythritol-4-phosphate pathway in Arabidopsis. *Plant Physiology* **124,** 95–103.

Estévez JM, Cantero A, Reindl A, Reichler S, Leòn P. 2001. 1-Deoxy-d-xylulose-5-phosphate synthase, a limiting enzyme for plastidic isoprenoid biosynthesis in plants. *Journal of Biological Chemistry* **276,** 22901–22909.

Flores-Pérez U, Sauret-Güeto S, Gas E, Jarvis P, Rodrìguez-Concepciòn M. 2008. A mutant impaired in the production of plastome-encoded proteins uncovers a mechanism for the homeostasis of isoprenoid biosynthetic enzymes in Arabidopsis plastids. *The Plant Cell* **20,** 1303–1315.

Gallois P, Marinho P. 1995. Leaf disc transformation using *Agrobacterium tumefaciens*—expression of heterologous genes in tobacco. *Methods in Molecular Biology* **49,** 39–48.

Guevara-García A, San Roman C, Arroyo A, Cortes M, de la Luz Gutierrez-Nava M, Leon P. 2005. Characterization of the Arabidopsis *clb6* mutant illustrates the importance of posttranscriptional regulation of the methyl-d-erythritol 4-phosphate pathway. *The Plant Cell* **17,** 628–643.

Gunata Y, Bayonove C, Baumes R. 1985. The aroma of grapes I. Extraction and determination of free and glycosidically bound fractions of some grape aroma components. *Journal of Chromatography A* **331,** 83–90.

Hahn F, Eubanks L, Testa C, Blagg B, Baker J, Poulter C. 2001. 1-Deoxy-d-xylulose 5-phosphate synthase, the gene product of open reading frame ORF 2816 and ORF 2895 in *Rhodobacter capsulatus*. *Journal of Bacteriology* **183,** 1–11.

Heymann H, Noble A. 1987. Descriptive analysis of commercial Cabernet Sauvignon wines from California. *American Journal of Enology and Viticulture* **38,** 41–44.

Hoballah ME, Stuurman J, Turlings TCJ, Guerin PM, Connétable S, Kuhlemeier C. 2005. The composition and timing of flower odour emission by wild *Petunia axillaris* coincide with the antennal perception and nocturnal activity of the pollinator Manduca sexta. *Planta* **222,** 141–150.

Hood E, Gelvin S, Melchers L, Hoekema A. 1993. New *Agrobacterium* helper plasmids for gene transfer to plants. *Transgenic Research* **2,** 208–218.

Jeong S, Hahn Y, Rong Q, Pfeifer K. 2007. Accurate quantitation of allele-specific expression patterns by analysis of DNA melting. *Genome Research* **17,** 1093–1100.

Karimi M, Inzé D, Depicker A. 2002. GATEWAY™ vectors for *Agrobacterium*-mediated plant transformation. *Trends in Plant Science* **7,** 193–195.

Kelley L, Sternberg M. 2009. Protein structure prediction on the Web: a case study using the Phyre server. *Nature Protocols* **4,** 363–371.

Kim B, Kim S, Chang Y. 2005. Differential expression of three 1-deoxy-d-xylulose-5-phosphate synthase genes in rice. *Biotechnology Letters* **27,** 997–1001.

Kuzuyama T, Takagi M, Takahashi S, Seto H. 2000. Cloning and characterization of 1-deoxy-d-xylulose 5-phosphate synthase from *Streptomyces* sp. strain CL190, which uses both the mevalonate and nonmevalonate pathways for isopentenyl diphosphate biosynthesis. *Journal of Bacteriology* **182,** 891–897.

Laule O, Fürholz A, Chang H-S, Zhu T, Wang X, Heifetz PB, Gruissem W, Lange M. 2003. Crosstalk between cytosolic and plastidial pathways of isoprenoid biosynthesis in. *Arabidopsis thaliana. Proceedings of the National Academy of Sciences, USA* **100,** 6866–6871.

Lewinsohn E, Schalechet F, Wilkinson J, *et al*. 2001. Enhanced levels of the aroma and flavour compound S-linalool by metabolic engineering of the terpenoid pathway in tomato fruits. *Plant Physiology* **127,** 1256–1265.

Lois LM, Campos N, Putra SR, Danielsen K, Rohmer M, Boronat A. 1998. Cloning and characterization of a gene from *Escherichia coli* encoding a transketolase-like enzyme that catalyzes the synthesis of D-1-deoxyxylulose 5-phosphate, a common precursor for isoprenoid, thiamin, and pyridoxol biosynthesis. *Proceedings of the National Academy of Sciences, USA* **95,** 2105–2110.

Luan F, Wüst M. 2002. Differential incorporation of 1-deoxy-d-xylulose into (3S)-linalool and geraniol in grape berry exocarp and mesocarp. *Phytochemistry* **60,** 451–459.

Lücker J, Bouwmeester HJ, Schwab W, Blaas J, van der Plas LHW, Verhoeven HA. 2001. Expression of *Clarkia S*-linalool synthase in transgenic petunia plants results in the accumulation of *S*-linalyl-β-glucopyranoside. *The Plant Journal* **27,** 315–324.

Lund ST, Bohlmann J. 2006. The molecular basis for wine grape quality—a volatile subject. *Science* **311,** 804–805.

Mandel MA, Feldmann KA, Herrera-Estrella L, Rocha-Sosa M, León P. 1996. *CLA1*, a novel gene required for chloroplast development, is highly conserved in evolution. *The Plant Journal* **9,** 649–658.

Mateo JJ, Jiménez M. 2000. Monoterpenes in grape juice and wines. *Journal of Chromatography A* **881,** 557–567.

Munoz-Bertomeu J, Arrillaga I, Ros R, Segura J. 2006. Up-regulation of 1-deoxy-D-xylulose-5-phosphate synthase enhances production of essential oils in transgenic Spike Lavender. *Plant Physiology* **142,** 890–900.

Pfaffl MW, Horgan GW, Dempfle L. 2002. Relative expression software tool REST. for group-wise comparison and statistical analysis of relative expression results in real-time PCR. *Nucleic Acids Research* **30,** 36.

Querol J, Besumbes O, Maria Lois L, Boronat A, Imperial S. 2001. A fluorometric assay for the determination of 1-deoxy-D-xylulose 5-phosphate synthase activity. *Analytical Biochemistry* **296,** 101–105.

Reid K, Olsson N, Schlosser J, Peng F, Lund S. 2006. An optimized grapevine RNA isolation procedure and statistical determination of reference genes for real-time RT-PCR during berry development. *BMC Plant Biology* **6,** 27.

Rodríguez-Villalón A, Gas E, Rodríguez-Concepción M. 2009. Phytoene synthase activity controls the biosynthesis of carotenoids and the supply of their metabolic precursors in dark-grown Arabidopsis seedlings. *The Plant Journal* **60,** 424–435.

Sauret-Güeto S, Botella-Pavía P, Flores-Pérez U, Martínez-García JF, San Román C, León P, Boronat A, Rodríguez-Concepción M. 2006. Plastid cues posttranscriptionally regulate the accumulation of key enzymes of the methylerythritol phosphate pathway in Arabidopsis. *Plant Physiology* **141,** 75–84.

Sprenger G, Schörken U, Wiegert T, Grolle S, de Graaf AA, Taylor SV, Begley TP, Bringer-Meyer S, Sahm H. 1997. Identification of a thiamin-dependent synthase in *Escherichia coli* required for the formation of the 1-deoxy-D-xylulose 5-phosphate precursor to isoprenoids, thiamin, and pyridoxol. *Proceedings of the National Academy of Sciences, USA* **94,** 12857–12862.

Strauss CR, Wilson B, Anderson R, Williams P. 1987. Development of precursors of C13 nor-isoprenoid flavorants in Riesling grapes. *American Journal of Enology and Viticulture* **38,** 23–27.

Strauss CR, Wilson B, Gooley PR, Williams PJ. 1986. Role of monoterpenes in grape and wine flavor. In: Parliment TH, Croteau R,

eds. *ACS Symposium Series 317*. Washington, DC: American Chemical Society, 222–242.

Trapp S, Croteau R. 2001. Defensive resin biosynthesis in Conifers. *Annal Review of Plant Physiology and Plant Molecular Biology* **52,** 689–724.

Versini G, Dalla Serra A, Monetti A, De Micheli L, Mattivi F. 1993. Free and bound grape aroma profiles variability within the family of muscat-called varieties. In: Bayonove C, Crouzet J, Flanzy C, Martin JC, Sapis JC, eds. *Proceedings of the International Symposium 'Connaissance aromatique des cecpages et qualitec des vins'*. Montpellier France,9–10 February, 1993.Revue Française d'Oenologie Lattes,12–21.

Wilson B, Strauss C, Williams P. 1984. Changes in free and glycosidically bound monoterpenes in developing muscat grapes. *Journal of Agricultural and Food Chemistry* **32,** 919–924.

Wilson B, Strauss CR, Williams PJ. 1986. The distribution of free and glycosidically-bound monoterpenes among skin, juice, and pulp fractions of some white grape varieties. *American Journal of Enology & Viticulture* **37,** 107–111.

Wolfertz M, Sharkey T, Boland W, Kuhnemann F. 2004. Rapid regulation of the methylerythritol 4-phosphate pathway during isoprene synthesis. *Plant Physiology* **135,** 1939.

Xiang S, Usunow G, Lange G, Busch M, Tong L. 2007. Crystal structure of 1-deoxy-d-xylulose 5-phosphate synthase, a crucial enzyme for isoprenoids biosynthesis. *Journal of Biological Chemistry* **282,** 2676–2682.

Yin S, Ding F, Dokholyan N. 2007. Eris: an automated estimator of protein stability. *Nature Methods* **4,** 466–467.

Yin S, Ding F, Dokholyan N. 2010. Computational evaluation of protein stability change upon mutations. *Methods in Molecular Biology* **634,** 189–201.

Zhang Y. 2008. I-TASSER server for protein 3D structure prediction. *BMC Bioinformatics* **9,** 40.